



The Combination of CD8 $\alpha\alpha$ and Peptide-MHC-I in a Face-to-Face Mode Promotes Chicken $\gamma\delta$ T Cells Response

Yanjie Liu^{1,2}, Rong Chen¹, Ruiying Liang¹, Beibei Sun¹, Yanan Wu¹, Lijie Zhang¹, Jim Kaufman^{3,4*} and Chun Xia^{1*}

OPEN ACCESS

Edited by:

Janice C. Telfer,
University of Massachusetts Amherst,
United States

Reviewed by:

Gregory Todd Pharr,
Mississippi State University,
United States
Jodi L. McGill,
Iowa State University, United States

*Correspondence:

Chun Xia
xiachun@cau.edu.cn
Jim Kaufman
jfk31@cam.ac.uk

Specialty section:

This article was submitted to
Comparative Immunology,
a section of the journal
Frontiers in Immunology

Received: 11 September 2020

Accepted: 27 October 2020

Published: 23 November 2020

Citation:

Liu Y, Chen R, Liang R, Sun B, Wu Y,
Zhang L, Kaufman J and Xia C (2020)
The Combination of CD8 $\alpha\alpha$ and
Peptide-MHC-I in a Face-to-Face
Mode Promotes Chicken $\gamma\delta$ T
Cells Response.
Front. Immunol. 11:605085.
doi: 10.3389/fimmu.2020.605085

¹ Department of Microbiology and Immunology, College of Veterinary Medicine, China Agricultural University, Beijing, China, ² Key Laboratory for Insect-Pollinator Biology of the Ministry of Agriculture, Institute of Apicultural Research, Chinese Academy of Agricultural Sciences, Beijing, China, ³ Department of Pathology, University of Cambridge, Cambridge, United Kingdom, ⁴ Department of Veterinary Medicine, University of Cambridge, Cambridge, United Kingdom

The CD8 $\alpha\alpha$ homodimer is crucial to both thymic T cell selection and the antigen recognition of cytotoxic T cells. The CD8-pMHC-I interaction can enhance CTL immunity *via* stabilizing the TCR-pMHC-I interaction and optimizing the cross-reactivity and Ag sensitivity of CD8⁺ T cells at various stages of development. To date, only human and mouse CD8-pMHC-I complexes have been determined. Here, we resolved the pBF2*1501 complex and the cCD8 $\alpha\alpha$ /pBF2*1501 and cCD8 $\alpha\alpha$ /pBF2*0401 complexes in nonmammals for the first time. Remarkably, cCD8 $\alpha\alpha$ /pBF2*1501 and the cCD8 $\alpha\alpha$ /pBF2*0401 complex both exhibited two binding modes, including an “antibody-like” mode similar to that of the known mammal CD8/pMHC-I complexes and a “face-to-face” mode that has been observed only in chickens to date. Compared to the “antibody-like” mode, the “face-to-face” binding mode changes the binding orientation of the cCD8 $\alpha\alpha$ homodimer to pMHC-I, which might facilitate abundant $\gamma\delta$ T cells to bind diverse peptides presented by limited BF2 alleles in chicken. Moreover, the forces involving in the interaction of cCD8 $\alpha\alpha$ /pBF2*1501 and the cCD8 $\alpha\alpha$ /pBF2*0401 are different in this two binding model, which might change the strength of the CD8-pMHC-I interaction, amplifying T cell cross-reactivity in chickens. The coreceptor CD8 $\alpha\alpha$ of TCR has evolved two peptide-MHC-I binding patterns in chickens, which might enhance the T cell response to major or emerging pathogens, including chicken-derived pathogens that are relevant to human health, such as high-pathogenicity influenza viruses.

Keywords: chicken $\gamma\delta$ T cells response, CD8/pMHC-I interaction, face-to-face mode, cCD8 $\alpha\alpha$ /pBF2*1501, cCD8 $\alpha\alpha$ /pBF2*0401

INTRODUCTION

Critical molecules involved in immune defense can be subject to an evolving molecular arms race with all kinds of pathogens, of which the most famous has led to the multiple loci, high allelic polymorphism and high sequence diversity of major histocompatibility complex (MHC) genes (1). These genes encode the classical class I and class II (aka MHC-I/II) molecules that bind antigenic peptides and present them for recognition by the T cell receptor (TCR) on T lymphocytes bearing coreceptors CD8 and CD4, respectively (2). TCR and CD8 cooperatively bind to the peptide-MHC-I complex (aka CD8-pMHC-I), which amplifies the peptide discrimination (3). The CD8-pMHC-I interaction enhances cytotoxic T lymphocyte immunity (4, 5) *via* stabilizing the TCR-pMHC-I interaction (6), recruiting essential signaling molecules to the intracellular side of the TCR-CD3 complex and locating the TCR to specific membrane domains at the cell surface (7–11). Over one million different peptides could be presented by a single classical MHC class I molecule and recognized by a single TCR *via* T cell cross-reactivity, a crucially important phenomenon in immune surveillance (12, 13). In addition, the CD8-pMHC-I interaction extends the range of pMHC-I ligands and is necessary to control the optimal T cell cross-reactivity (14). Indeed, an enhanced level of T cell cross-reactivity in mice was predicted on theoretical grounds (13) because of stronger CD8-pMHC-I interaction than in humans. However, the multiple structural basis of T cell cross-reactivity has now been explained, focusing on the interaction between TCR and pMHC-I and the characteristics of peptide binding (15).

In representative mammals such as humans and mice, only two nonpolymorphic CD8 genes are found, CD8A and CD8B (16). The CD8 dimer exists as a glycoprotein on the T cell surface in two isoforms, CD8 $\alpha\alpha$ and CD8 $\alpha\beta$. According to current knowledge of human and mouse immunology, CD8 α is mainly expressed on the surface of $\gamma\delta$ T cells, natural killer (NK) cells and dendritic cells (DCs) (17). Despite the different isoforms, CD8 $\alpha\alpha$ and CD8 $\alpha\beta$ show similar affinity for pMHC-I, and both CD8 $\alpha\alpha$ and CD8 $\alpha\beta$ interact with pMHC-I and promote TCR-pMHC-I recognition (18, 19). The chicken is the best-characterized nonmammalian model in terms of immunology (20). Both chicken CD8 $\alpha\beta$ and CD8 $\alpha\alpha$ dimers are found on similar cells to those in mammals (21–24). In comparison with the known human and mouse CD8 α proteins, chicken CD8 α (cCD8 α) showed lower diversity in the CDR1-like loop and the CDR2-like loop caused by mutation of their specific amino acid sequences (25, 26). In addition, cCD8 $\alpha\alpha$ maintains a few conserved residues with respect to the interaction of human and mouse CD8 $\alpha\alpha$ with pMHC-I (26). In contrast to the lower $\gamma\delta$ T cell numbers in human and mouse (27, 28), CD8 $^+\gamma\delta$ T cells represent a major cytotoxic lymphocyte (CTL) subset appearing in the peripheral blood as well as organs such as the gut, spleen, thymus, and bursa of Fabricius of chicken (29–31), constituting up to 50% of peripheral T cells (32, 33). Indeed, after pathogenic bacteria infection, CD8 $\alpha\alpha^+$ $\gamma\delta$ T cell subsets in the spleen, caecum and blood were expanded, further performing CTL immunobiological function (34).

To date, only human and mouse CD8-pMHC-I interactions have been determined; that is, the structures of hCD8 $\alpha\alpha$ /HLA-A*0201, hCD8 $\alpha\alpha$ /HLA-A*2402, mCD8 $\alpha\alpha$ /H-2K^b and mCD8 $\alpha\beta$ /H-2D^d have been resolved (19, 35–37). These CD8/pMHC-I structures reveal that CD8 binds to the protruding pMHC-I α 3 domain CD loop in an antibody-like manner. Human and mouse CD8 interact with pMHC-I in an allele-dependent but TCR- and peptide-independent manner (38, 39). However, CD8 engagement guides the geometry of TCR-pMHC-I recognition to achieve the intracellular juxtaposition of coreceptor-bound Lck with CD3 ITAMs (34, 40). However, to date, there is still a lack of information on the nonmammalian CD8/pMHC-I complex structure.

In the first comparative analysis, only two residues on the surface of the chicken class I α 3 domain were found to be identical with those in mammals, which led to a proposal for the contact site for CD8 binding (41), now amply confirmed by mutagenesis, structural analysis and biophysical analysis in humans and mice (35–37, 42–44). In addition, the chicken class I α 3 domain displays moderate levels of allelic polymorphism and sequence diversity (25, 45), suggesting a complementary selective pressure for diversity in the ligand for the polymorphic and polygenic chicken CD8A system. Of further interest is the fact that only the classical class I gene BF2 is expressed at a high level in chickens, and chickens can live or die based on whether pathogen peptides are bound and presented by the dominantly expressed class I molecule (46–48), intensifying the selection for appropriate CD8 binding.

In this paper, we determined amazingly high affinities between chicken CD8 $\alpha\alpha$ homodimers and pBF2*1501 compared to mammalian CD8-pMHC-I interactions and derived cocrystals of chicken CD8 $\alpha\alpha$ homodimers with pBF2*1501 and pBF2*0401. We first confirmed that CD8 dimers recognize the same CD loop of the α 3 domain in two different modes, namely, an “antibody-like” mode and a “face-to-face” mode that does not occur in mammals. The two binding models are very helpful to the understanding of chicken T cell immunity, including the limited MHC-I allelic genes and added specific T cell constituents. In addition, the two binding modes may have developed due to the molecular arms race with major or emerging pathogens, including chicken-derived pathogens that are relevant to human health, such as highly variable and highly pathogenic influenza virus strains.

MATERIALS AND METHODS

Protein Preparation

The peptide RY0808 (RRREQTDY) derived from MDV was synthesized by Invitrogen, USA. The pET21a plasmids encoding chicken CD8 α , BF2*1501, BF2*0401, and β 2m and another peptide termed IE8 (IDWFDGKE) for prokaryotic expression were maintained in our laboratory (26, 49, 50). Proteins of chicken CD8 α (cCD8 α), BF2*1501, BF2*0401, and β 2m were expressed as inclusion bodies, and the preparation of soluble cCD8 α protein was carried out essentially as described previously (26). The cCD8 $\alpha\alpha$ protein was purified on a

Superdex 200 16/60 column (GE Healthcare, USA). In addition, after the refolding of BF2*1501 and β 2m with RY0808 and of BF2*0401 and β 2m with the IE8 peptide, the refolded complexes were further purified on a Superdex 200 16/60 column, followed by Resource Q anion-exchange chromatography (GE Healthcare, USA). The purified RY0808-BF2*1501- β 2m (pBF2*1501) and IE8-BF2*0401- β 2m (pBF2*0401) complexes were buffer-exchanged three times with 10 mM Tris-HCl, 50 mM NaCl, pH 8.0. Next, pBF2*1501, the cCD8 $\alpha\alpha$ and pBF2*1501 (cCD8 $\alpha\alpha$ /pBF2*1501) complexes and the cCD8 $\alpha\alpha$ and pBF2*0401 complexes (cCD8 $\alpha\alpha$ /pBF2*0401) were mixed at a 2:1 molar ratio at 277 K overnight. Finally, the chicken protein complexes pBF2*1501, cCD8 $\alpha\alpha$ /pBF2*1501, and cCD8 $\alpha\alpha$ /pBF2*0401 were diluted to 5 mg ml⁻¹ and 10 mg ml⁻¹.

Affinity Analysis by Surface Plasmon Resonance and Superdex75 16/60 Column

Surface plasmon resonance binding experiments were performed on a Biacore3000. pBF2*1501 and cCD8 $\alpha\alpha$ protein both were purified with buffer containing 10mM HEPES PH 7.4, 150mM NaCl, 3mM EDTA and 0.005% Tween 20. pBF2*1501 was covalently coupled with CM-5 chip (cat. no. BR-1000-14, Biacore-GE Healthcare, Piscataway, NJ) as the stationary phase. The different concentration of cCD8 $\alpha\alpha$ including 0, 0.78, 1.56, 3.125, 6.25, 12.5, 25, and 50 μ M were injected as the mobile phase. And then, the data were analyzed with BIA Evaluation Software 3.2. The coupling conditions and data analysis were performed as described previously (51). After the incubation of purified cCD8 $\alpha\alpha$ and pBF2*1501 for 3 h at 4°C, the coexistence of chicken cCD8 $\alpha\alpha$ and pBF2*1501 complexes on the gel column was tested by using a Superdex 75 16/60 column (GE Healthcare, USA) and sodium dodecyl sulfate-polyacrylamide gel electrophoresis (SDS-PAGE).

Crystallization and Data Collection

The complexes pBF2*1501, cCD8 $\alpha\alpha$ /pBF2*1501 and cCD8 $\alpha\alpha$ /pBF2*0401 were screened in crystallization trials by the sitting-drop vapor-diffusion method with the Index, Crystal Screen, Crystal Screen 2, Crystal Screen Cryo, Crystal Screen 2 Cryo, and PEG Ion 1 and 2 Kits (Hampton Research, USA) at 291 K. Crystals from the protein concentration of 10 mg ml⁻¹ were observed in PEG Ion Kit No. 16 (0.2 M magnesium nitrate hexahydrate, 20% (w/v) polyethylene glycol 3,350, pH 5.8) and Index Kit No. 72 (0.2 M sodium chloride, 25% (w/v) polyethylene glycol 3,350, 0.1 M HEPES pH 7.5) and No. 67 (0.2 M ammonium sulfate, 0.1 M Bis-tris pH 6.5, 25% (w/v) polyethylene glycol 3,350). Diffraction data from chicken pBF2*1501, cCD8 $\alpha\alpha$ /pBF2*1501 and cCD8 $\alpha\alpha$ /pBF2*0401 complexes were collected on Beamline BL17U at the Shanghai Synchrotron Radiation Facility (SSRF; Shanghai, People's Republic of China) at a wavelength of 0.97972 Å with an ADSC Q315 CCD detector. The collected diffraction data were indexed and scaled with HKL2000 (52).

Structure Determination and Refinement

The structures were determined by molecular replacement by using Molrep and Phaser in the CCP4 package, with the structures of chicken CD8 $\alpha\alpha$ [Protein Data Bank (PDB) code:

5EB9] and BF2*0401-IE8 [PDB code: 4E0R] as the search models. The construction and refinement of the complex were performed by the programs Coot and Refmac5. Subsequent refinements were conducted for energy minimization, the restriction of individual B factors, and the addition of water molecules, with noncrystallographic symmetry restraints applied to the one molecule of pBF2*1501 and the two molecules of chicken cCD8 $\alpha\alpha$ /pBF2*1501 and cCD8 $\alpha\alpha$ /pBF2*0401 in the asymmetric unit. Ramachandran plots and secondary structure assignments were generated by SFCHECK (53). The final structures of the complex consisted of pBF2*1501 and two complete chicken cCD8 $\alpha\alpha$ /pBF2*1501 and cCD8 $\alpha\alpha$ /pBF2*0401 molecules, with R-factor = 0.2304, R-free = 0.2647; R-factor = 0.2533, R-free = 0.2990; and R-factor = 0.2519, R-free = 0.2881, respectively. These crystal structures of cCD8 $\alpha\alpha$ /pBF2*1501, cCD8 $\alpha\alpha$ /pBF2*0401, and pBF2*1501 have been deposited in the PDB (<http://www.pdb.org/pdb/home/home.do>) with accession numbers 6LHF, 6LHG and 6LHH.

Structural Analysis and Generation of Illustrations

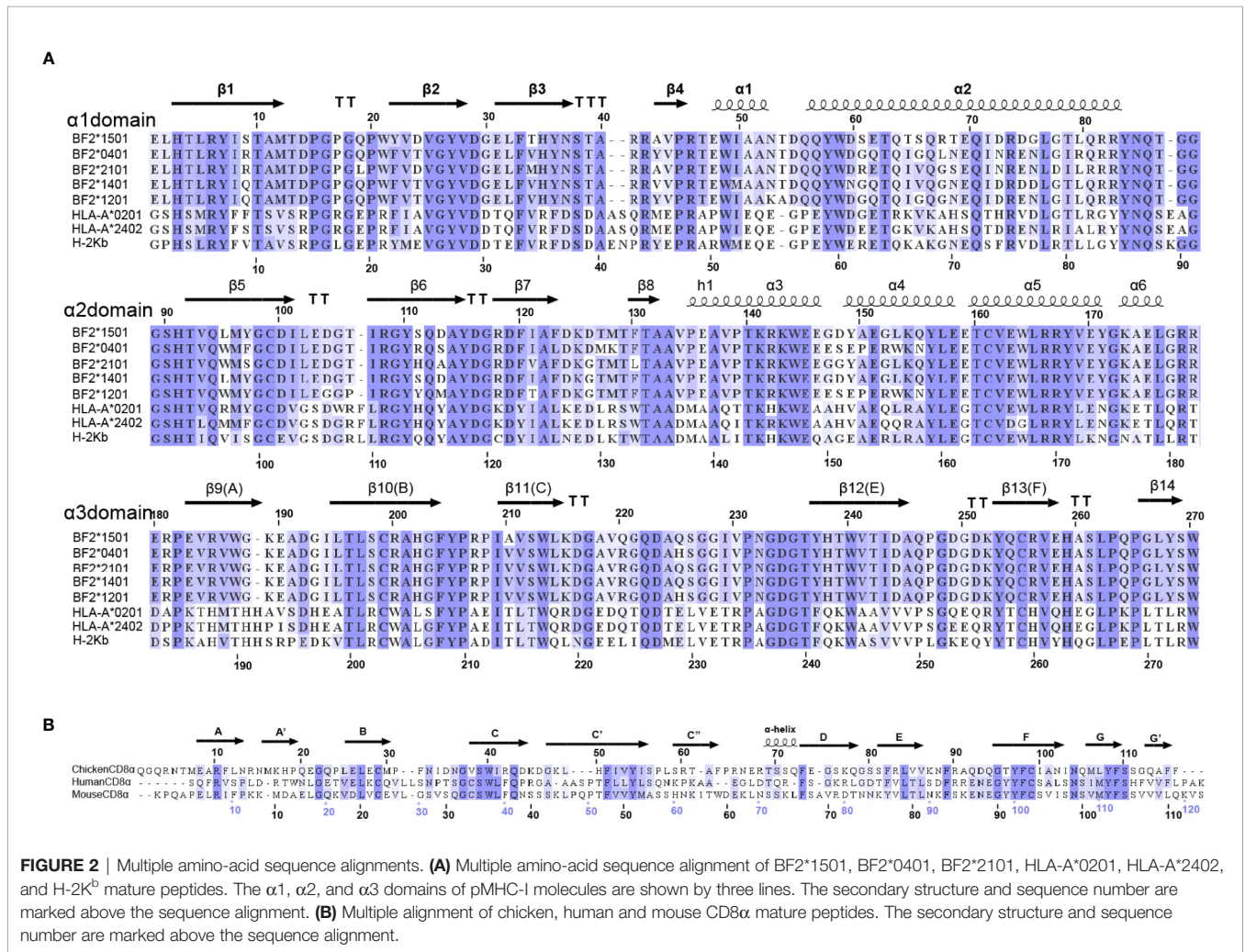
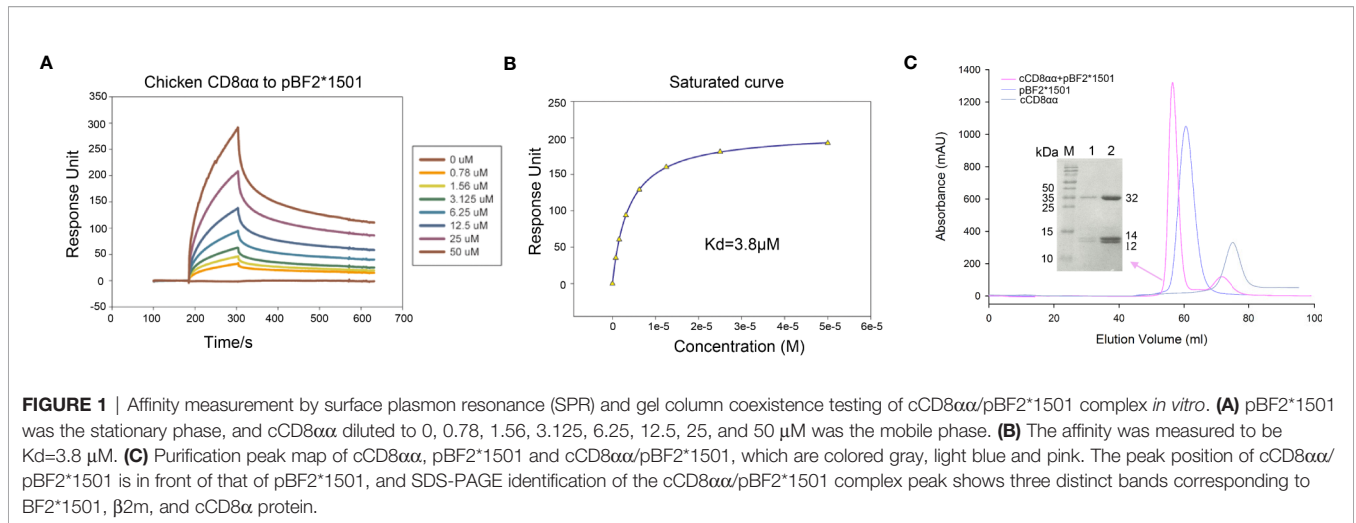
The residues involved in the interactions of cCD8 $\alpha\alpha$ with pBF2*1501 and pBF2*0401 were identified by the web servers PDBePISA (<https://www.ebi.ac.uk/pdbe/pisa/>) (13) and Ring (<http://protein.bio.unipd.it/ring/>) (12). Structural illustrations and electrostatic potential surfaces were generated with the PyMOL molecular graphics system (DeLano Scientific; <http://www.pymol.org>).

RESULTS

An Unexpected Interaction Exists Between cCD8 $\alpha\alpha$ and pBF2*1501

The affinity between cCD8 $\alpha\alpha$ and pBF2*1501 (K_d=3.8 μ M) is higher than the known binding of CD8 and pMHC-I in mammals (54) (Figures 1A, B). Additionally, cCD8 $\alpha\alpha$ and pBF2*1501 can stably coexist on a gel column *in vitro* (Figure 1C). In addition, the amino acids of chicken BF2 molecules exhibited a large difference from those of humans and mice, especially for the α 3 domain, and only 28 conserved residues exist between the α 3 domains of BF2 molecules and HLA-A*0201 and mouse H-2K^b (Figure 2A). In addition, there were only 20 conserved residues between chicken CD8 α and human and mouse CD8 α (Figure 2B). Therefore, an unexpected interaction between chicken CD8 α and pMHC-I was distinct from those in humans and mice.

To investigate the interaction of CD8 and classical class I molecules in chickens, cocrystals of pBF2*1501 with peptide RRREQTDY (RY0808), of cCD8 $\alpha\alpha$ homodimers with the pBF2*0401 molecule and the peptide IDWFDGKE (IE8) were formed as previously reported (49), as well as cCD8 $\alpha\alpha$ homodimers with the pBF2*1501 molecule just described, which diffracted to 2.7 Å, 2.6 Å, and 2.8 Å and belonged to the P3₁2₁, P1, and P2₁ space groups, respectively (Table 1).



cCD8 $\alpha\alpha$ Binding Shows a “Pull” of the CD Loop of pMHC-I

The BF2*1501 complex consists of $\alpha 1$, $\alpha 2$, $\alpha 3$ domains of the heavy chain, a light chain $\beta 2m$, and the 8-mer peptide RRREQTDY (henceforth called RY0808), which is extremely similar to other known chicken class I molecules including BF2*2101 (3BEV), BF2*0401 (40ER), BF2*1401 (4CW1), BF2*1201 (5YMV) with C α root mean square deviations (RMSDs) value of 0.83 Å, 0.54 Å, 0.51 Å and 0.82 Å respectively; the complexes also share the closely similar $\alpha 3$ domain CD loop (Figure 3A). However, the chicken BF2 structures differ more from human, mouse, bovine, and swine MHC class I structures, with C α RMSD values of 2.61 Å, 2.11 Å, 1.98 Å, and 1.91 Å, especially for the $\alpha 3$ domain CD loops, which are shifted away from the human and mouse CD8 orientation by approximately 3.4–3.7 Å, which theoretically should result in a spatial relationship between cCD8 and the $\alpha 3$ domain of pMHC-I in chickens (Figure 3B). This different conformation of the $\alpha 3$ domain CD loop might lead to the distinct binding mode between CD8 and pMHC-I complexes in chickens and mammals because of the narrow space for CD8 engagement in chickens.

Similar to the human hCD8 $\alpha\alpha$ /pHLA-A*2402 and mouse mCD8 $\alpha\alpha$ /pH-2K^b complexes, each unit cell of cCD8 $\alpha\alpha$ /pBF2*1501 and cCD8 $\alpha\alpha$ /pBF2*0401 contained two asymmetric complexes, each with one class I heterotrimer (RY0808/BF2*1501/ $\beta 2m$ and IE8/BF2*0401/ $\beta 2m$) and one

CD8 $\alpha\alpha$ homodimer, termed complex A and complex B (Figure 4). In addition, cCD8 $\alpha\alpha$ binding did not change the main chain of the peptides, except that some side chains of the nonanchoring peptide residues became flexible in both the cCD8 $\alpha\alpha$ /pBF2*0401 and cCD8 $\alpha\alpha$ /pBF2*1501 complexes, which did not alter the peptide binding to BF2*1501, BF2*0401 and the corresponding TCR (Figures 3C and S1A). However, compared to the pBF2*1501 complex, the $\alpha 3$ domain CD loop of complex A and complex B with intact mesh were pulled towards cCD8 $\alpha\alpha$ by approximately 4.2 Å and 3.8 Å in the cCD8 $\alpha\alpha$ /pBF2*1501 complex. Complexes A and B of cCD8 $\alpha\alpha$ /pBF2*0401 also moved towards cCD8 $\alpha\alpha$ by approximately 4.3 Å and 4.0 Å (Figures 3C and S1B). Moreover, the crucial protruding $\alpha 3$ domain CD loop differs in direction, and the protruding loop (220–228) in the CD loop of the $\alpha 3$ domain is an important region for CD8 binding independent of species (43, 55, 56) (Figure 3C). This phenomenon is completely different from the “pull” and “push” binding of the MHC-I $\alpha 3$ domain CD loop adopted by complexes A and B, respectively, in humans and mice (35, 36).

Chicken cCD8 $\alpha\alpha$ /pMHC-I Complexes Demonstrate Two Different cCD8 $\alpha\alpha$ Engagement Modes

The CD loop of complex B lies closer to the cCD8 $\alpha\alpha$ homodimer, and the whole cCD8 $\alpha\alpha$ homodimer clearly skews towards the $\alpha 2$ domain and $\beta 2m$ in complex A compared to complex B (Figure 5). The hCD8 $\alpha\alpha$ /pHLA-A*0201, hCD8 $\alpha\alpha$ /pHLA-A*2402 and mCD8 $\alpha\alpha$ /pH-2K^b complexes proved that the CD loop of $\alpha 3$ domain forms hydrogen bonds and salt bridges with CD8 $\alpha\alpha$. The $\alpha 3$ domain CD loop is clamped by all six CDR-like loops of CD8 $\alpha\alpha$, among which Gln226 is the most important residue and is conserved across different species.

In cCD8 $\alpha\alpha$ /pBF2*1501 complex A, the corresponding residue Gln222 only forms two hydrogen bonds with Asn102 on F strand and Gln105 on CDR3-like loop of the cCD8 $\alpha 1$ subunit and forms one hydrogen bond with Asn102 on F strand of the cCD8 $\alpha 2$ subunit instead of the conserved C strand that located on the deep of CD8 cavity in humans and mice. Moreover, Ala224 of $\alpha 3$ domain CD loop forms one hydrogen bond with Gln105 of the cCD8 $\alpha 1$ CDR3-like loop, and Asp223 of $\alpha 3$ domain CD loop forms one hydrogen bond with Tyr54 of the cCD8 $\alpha 2$ C' strand in complex A (Figure 5A). Besides that, four water molecules participate in the interactions and forms a forces network between $\alpha 3$ domain CD loop and cCD8 α subunits (Figure 5A). In cCD8 $\alpha\alpha$ /pBF2*0401 complex A, the corresponding residue Gln222 only forms one hydrogen bond with Gln105 on CDR3-like loop of the cCD8 $\alpha 1$ subunit. Another two hydrogen bonds are formed between Val219 and Ser226 of $\alpha 3$ domain CD loop and Asn104 of the cCD8 $\alpha\alpha$ CDR3-like loop, and Asp223 of $\alpha 3$ domain CD loop forms one hydrogen bond with Tyr54 of the cCD8 $\alpha 2$ C' strand in complex A (Figure 5B). Therefore, Gln222 of BF2*1501 and BF2*0401 $\alpha 3$ domain CD loops is not a significant residue, which inserts into the deep of CD8 cavity and contribute to the antibody-like interaction model existing in the human and mouse CD8/pMHC-I complex. The corresponding residue Gln226 in the

TABLE 1 | X-ray diffraction data processing and refinement statistics.

Statistic Value for:	cCD8 $\alpha\alpha$ /pBF2*0401	cCD8 $\alpha\alpha$ /pBF2*1501	BF2*1501/RY0808
Data processing			
Space group	P2 ₁	P1	P3 ₁ 2 ₁
Cell parameters			
a (Å)	90.576	51.34	123.45
b (Å)	90.82	66.73	123.45
c (Å)	94.87	103.95	81.22
α (°)	90.00	84.60	90.00
β (°)	98.61	82.04	90.00
γ (°)	90.00	67.51	120.00
Resolution range (Å)	50.00–2.80 (2.90–2.80)	50.00–2.6 (2.69–2.6)	50.00–2.71 (2.77–2.71)
Total reflections	163307	108500	111237
Unique reflections	37565	36586	18044
Completeness (%)	99.57 (97.75)	95.34 (93.09)	96.2(97.7)
Redundancy	4.3(4.5)	3.0(3.1)	3.4(2.1)
R _{merge} (%)	10.5(61.3)	10.9(51.6)	8.0(24.00)
I/ σ (I)	10.21 (3.04)	8.25 (3.24)	11.09(2.659)
Refinement			
R _{work}	0.2519	0.2533	0.2304
R _{free}	0.2881	0.2990	0.2647
RMSD			
Bond lengths (Å)	0.005	0.010	0.004
Bond angles (°)	1.16	1.68	0.865
Average B factor	80.60	58.40	59.58
Ramachandran plot			
Most favored (%)	97	96	97.1
Disallowed (%)	0.17	0	0

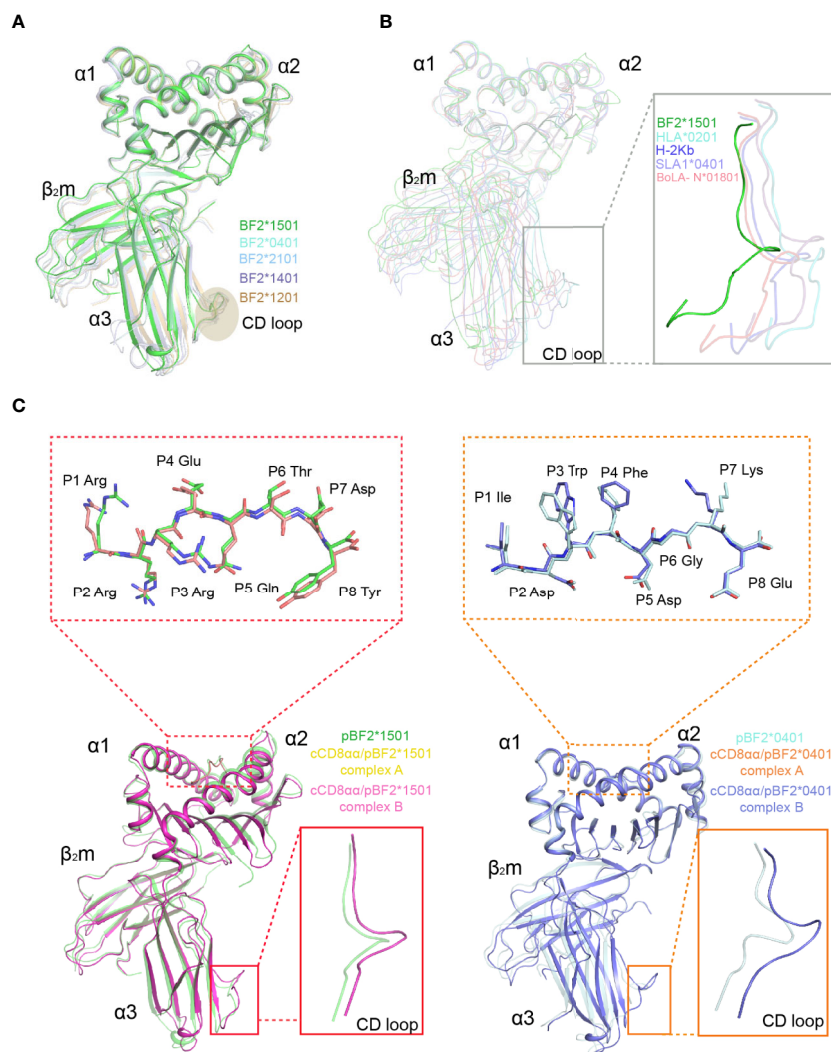


FIGURE 3 | Superposition of pBF2*1501 with other known chicken pMHC-I structures, representative mammalian pMHC-I structures and cCD8 α /pBF2*1501 and cCD8 α /pBF2*0401 complexes. **(A)** Superimposed C α traces of chicken BF2*1501-RY0808- β 2m (green), pBF2*0401 (PDB code: 4E0R, cyan), pBF2*2101 (PDB code: 3BEV, light blue), pBF2*1401 (PDB code: 4CW1, purple), and pBF2*1201 (PDB code: 5YMV, brown). **(B)** C α -trace comparison of BF2*1501-RY0808- β 2m (green), HLA-A*0201 (PDB code: 1HHK, cyan), H-2K^b (PDB code: 1G7Q, blue), SLA-1*0401 (PDB code: 3QQ3, light purple), and BoLA-N*01801 (PDB code: 3PWU, light red), with an enlarged view of the CD loop in the gray box. **(C)** Overlap between free pBF2*1501 and pBF2*1501 of cCD8 α /pBF2*1501 and between free pBF2*0401 and pBF2*0401 of cCD8 α /pBF2*0401, based on the α 1 and α 2 domains, respectively. Enlarged views of the overlapped peptides are shown in the dotted red box and dotted orange box for cCD8 α /pBF2*1501 and cCD8 α /pBF2*0401, respectively; an enlarged view of the overlapped α 3 domain CD loop is shown in the red box and orange box for cCD8 α /pBF2*1501 and cCD8 α /pBF2*0401. Free pBF2*1501, pBF2*1501 of cCD8 α /pBF2*1501 complex A, pBF2*1501 of cCD8 α /pBF2*1501 complex B, free pBF2*0401, pBF2*0401 of cCD8 α /pBF2*0401 complex A and pBF2*0401 of cCD8 α /pBF2*0401 complex B are colored green, yellow, light pink, cyan, orange, and light blue, respectively.

mammalian CD8 α /pMHC-I complex is the most important residue contributing to the antibody-like binding model of the mammalian CD8 α /pMHC-I complex (35–37). The special interaction contributed by important residue Gln222 and other distinct interactions between cCD8 α and the CD loop of the α 3 domain leads to the rotation of complex A towards the α 2 domain and β 2m in comparison to complex B, which finally creates a novel binding mode that we termed the “face-to-face” mode (Figure 5 and Table 2).

However, cCD8 α /pBF2*1501 complex B and cCD8 α /pBF2*0401 complex B present a parallel binding model of cCD8 α interaction with hCD8 α /pHLA-A*0201 and mCD8 α /pH-2K^b. In the CD loop of the pBF2*1501 α 3 domain, Ser226 forms one hydrogen bond with Asn104 of the CDR3-like loop of cCD8 α 1 subunit; Gln225 forms two hydrogen bonds with Asn104 of the CDR3-like loop of cCD8 α 1 subunit; Asp223 forms one hydrogen bond with Tyr54 of the cCD8 α 2 C' strand; Val219 forms two hydrogen bonds with Asn104 of the

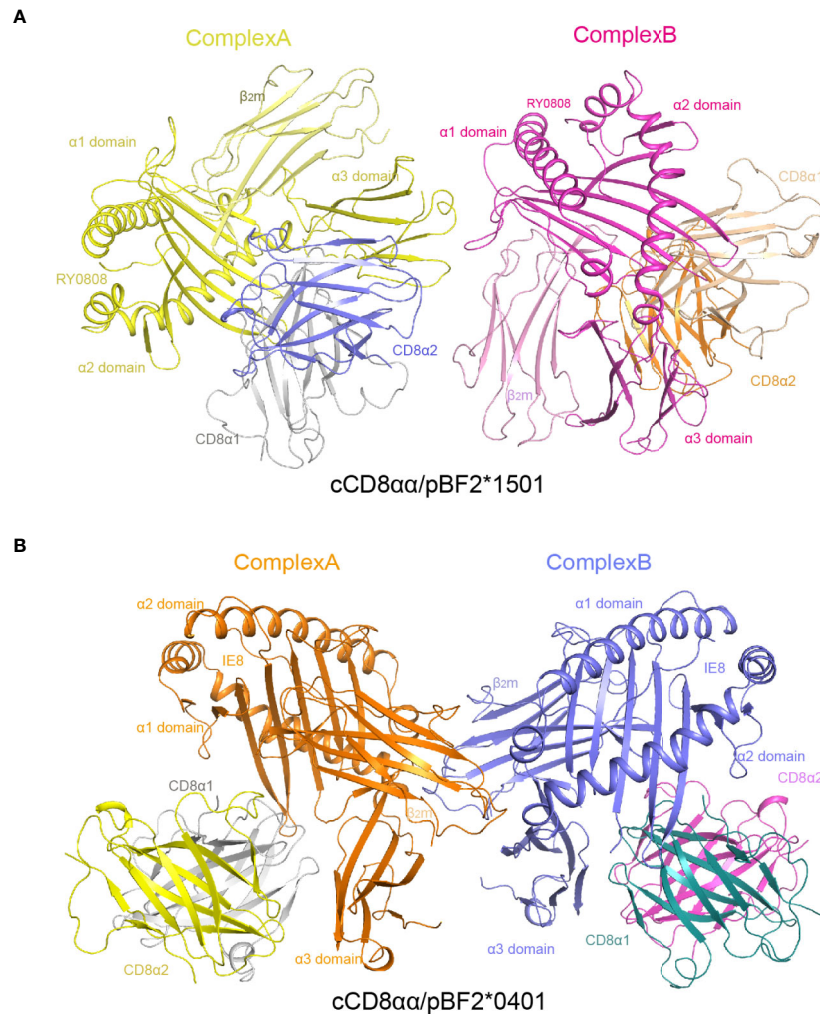


FIGURE 4 | Overall view of chicken cCD8 α /pBF2*1501 and cCD8 α /pBF2*0401 complexes. **(A)** An asymmetric unit contains two chicken cCD8 α /pBF2*1501 complexes, namely, complex A and complex B, each consisting of pBF2*1501 (BF2*1501, chicken $\beta 2m$, and the peptide RY0808) and the cCD8 $\alpha\alpha$ homodimer. pBF2*1501, the cCD8 $\alpha 1$ subunit, and the cCD8 $\alpha 2$ subunit of complex A are colored yellow, gray and blue, respectively. pBF2*1501, the cCD8 $\alpha 1$ subunit, and the cCD8 $\alpha 2$ subunit of complex B are colored pink, light brown and orange, respectively. **(B)** An asymmetric unit contains two chicken cCD8 α /pBF2*0401 complexes, namely, complex A and complex B, each consisting of pBF2*0401 (BF2*0401, chicken $\beta 2m$, and the peptide IE8) and the cCD8 $\alpha\alpha$ homodimer. pBF2*0401, the cCD8 $\alpha 1$ subunit, and the cCD8 $\alpha 2$ subunit of complex A are colored orange, gray and yellow, respectively. pBF2*0401, the cCD8 $\alpha 1$ subunit, and the cCD8 $\alpha 2$ subunit of complex B are colored blue, deep green, and pink, respectively.

cCD8 $\alpha 2$ CDR3-like loop, and the important residue Gln222 forms one hydrogen bond with Ser39 of the cCD8 $\alpha 2$ C strand and a water molecule participates in the stabilization of Gln222 (**Figure 5A**). In the pBF2*0401 $\alpha 3$ domain CD loop, in addition to two hydrogen bonds formed by Val219 with Asn104 of cCD8 $\alpha 2$, the Arg220 forms one hydrogen bond with Asp35 of cCD8 $\alpha 2$ CDR1-like loop, the Asp223 forms one hydrogen bond with Tyr54 of the cCD8 $\alpha 2$ C' strand, the Ser226 forms one hydrogen bond with Asn104 of the cCD8 $\alpha 1$ CDR3-like loop, and the protruding residue of Gln222 forms two hydrogen bonds with Ser39 of the cCD8 $\alpha 2$ C strand (**Figure 5B**). Thus, the two cCD8 α subunits clamp the CD loop, and the key residue Gln222 inserts into the deep of CD8 cavity and plays vital roles in the

interactions of complexes B, which is similar to the classical binding mode in mammalian CD8/pMHC-I complexes.

The “Face-to-Face” Mode Causes Different and Fewer Interactions in Complex A

In addition to those in the CD loop, other differences exist in the $\alpha 2$, $\beta 2m$ and $\alpha 3$ domains of cCD8 α /pBF2*1501 and cCD8 α /pBF2*0401 complexes A and B (**Figure 6** and **Supplementary Table 1**). In cCD8 α /pBF2*1501 complex A, Arg207 of the $\alpha 3$ domain BC loop forms one hydrogen bond and one salt bridge with Asp35 of the cCD8 $\alpha 1$ CDR-like loop (**Figure 6A**). However, in cCD8 α /pBF2*1501 complex B, one hydrogen

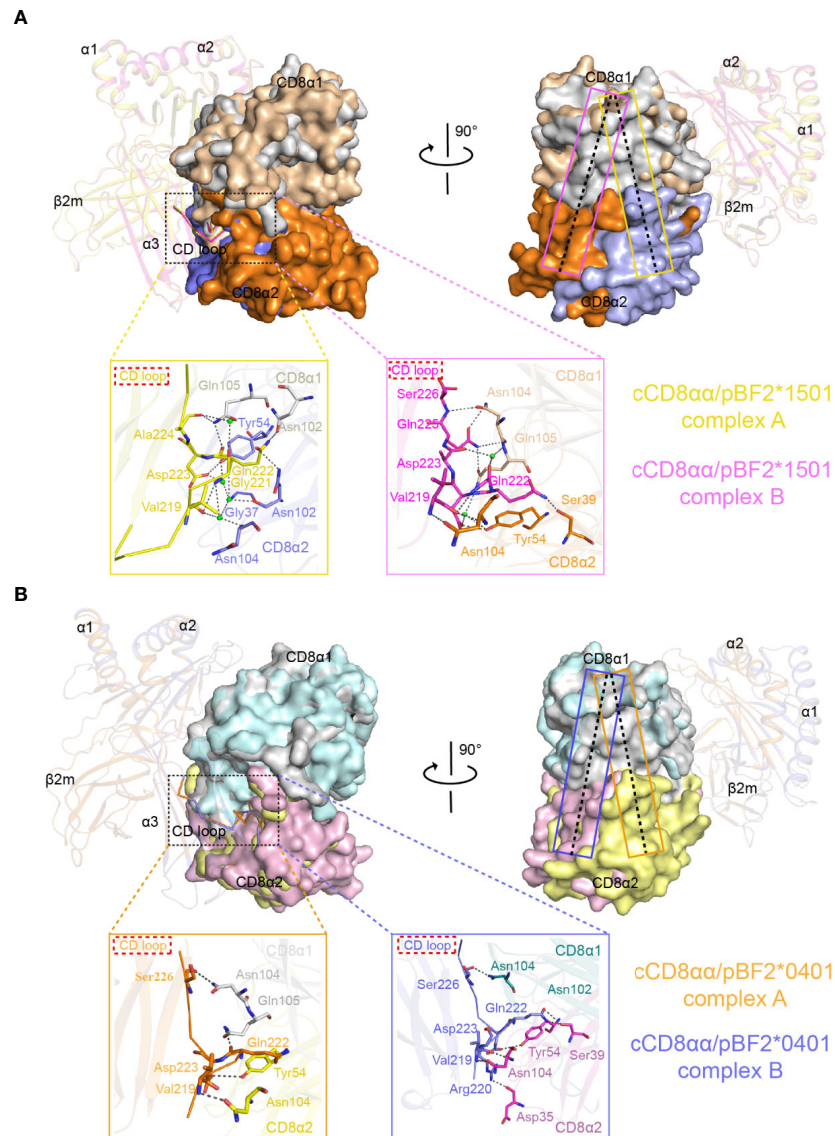


FIGURE 5 | Superposition of complex A and complex B of cCD8 $\alpha\alpha$ /pBF2*1501 and cCD8 $\alpha\alpha$ /pBF2*0401 using the C α atoms of domains α 1 and α 2. **(A)** Overlap of complex A and complex B of cCD8 $\alpha\alpha$ /pBF2*1501 based on the C α atoms of domains α 1 and α 2, as shown from the front view and in a clockwise rotation by 90°. The interaction details between the α 3 domain CD loop and the cCD8 $\alpha\alpha$ homodimer are shown in an enlarged view in yellow and pink boxes for complex A and complex B, respectively. In complex A, the contact residues are shown in stick representation, and the residues of BF2*1501 are colored yellow. The residues of cCD8 α 1 are colored gray, the residues of cCD8 α 2 are colored light blue, and the interaction forces are marked by black dotted lines. In complex B, the contact residues are shown in stick representation, and the residues of BF2*1501 are colored light pink. The residues of cCD8 α 1 are colored light brown, the residues of cCD8 α 2 are colored orange, and the interaction forces are marked by black dotted lines. pBF2*1501 of cCD8 $\alpha\alpha$ /pBF2*1501 complex A and cCD8 $\alpha\alpha$ /pBF2*1501 complex B are colored yellow and light pink; the cCD8 α 1 and cCD8 α 2 subunits of the cCD8 $\alpha\alpha$ /pBF2*1501 complex A are colored light gray and light blue; and the cCD8 α 1 and cCD8 α 2 subunits of cCD8 $\alpha\alpha$ /pBF2*1501 complex B are colored light brown and orange. The yellow and pink rectangles represent the central plane of the cCD8 $\alpha\alpha$ homodimer of complex A and complex B of cCD8 $\alpha\alpha$ /pBF2*1501, respectively. **(B)** Overlap of complex A and complex B of cCD8 $\alpha\alpha$ /pBF2*0401 based on the C α atoms of domains α 1 and α 2, shown from the front view and rotated clockwise by 90°. The interaction details between the α 3 domain CD loop and the cCD8 $\alpha\alpha$ homodimer are shown in enlarged views in light orange and light blue boxes for complex A and complex B, respectively. In complex A, the contact residues are shown in stick representation, and the residues of BF2*0401 are colored light orange, the residues of cCD8 α 2 are colored yellow, and the interaction forces are marked by black dotted lines. In complex B, the contact residues are shown in stick representation, the residues of BF2*0401 are colored light blue, the residues of cCD8 α 1 are colored deep green, the residues of cCD8 α 2 are colored pink, and the interaction forces are marked by black dotted lines. pBF2*0401 of cCD8 $\alpha\alpha$ /pBF2*0401 complex A and cCD8 $\alpha\alpha$ /pBF2*0401 complex B are colored light orange and light blue; the cCD8 α 1 and cCD8 α 2 subunits of cCD8 $\alpha\alpha$ /pBF2*0401 complex A are colored gray and yellow; and the cCD8 α 1 and cCD8 α 2 subunits of cCD8 $\alpha\alpha$ /pBF2*0401 complex B are colored deep-green and pink. The orange and blue rectangles represent the central plane of the cCD8 $\alpha\alpha$ homodimer of complex A and complex B of cCD8 $\alpha\alpha$ /pBF2*0401, respectively.

TABLE 2 | Statistics of forces in cCD8 $\alpha\alpha$ /pBF2*1501 and cCD8 $\alpha\alpha$ /pBF2*0401 complexes.

Forces	cCD8 $\alpha\alpha$ / BF2*1501 complex A	cCD8 $\alpha\alpha$ / BF2*1501 complex B	cCD8 $\alpha\alpha$ / BF2*0401 complex A	cCD8 $\alpha\alpha$ / BF2*0401 complex B
Hydrogen bonds (H)	7 H	12 H	8 H	11 H
Salt bridges (S)	1 S	1 S	2 S	1 S
Van der Waals (vdw)	27 vdw	34 vdw	11 vdw	14 vdw

bond was formed between Arg207 and Asp35, and Glu258 forms one salt bridge with Arg60 of cCD8 α 1, Lys215 forms one hydrogen bond with Asp35 of cCD8 α 2 (**Figure 6A**). In the cCD8 $\alpha\alpha$ /pBF2*0401 complex A, the corresponding residue Arg207 of the α 3 domain BC loop forms one hydrogen bond and one salt bridge with Asp35 of the cCD8 α 1 CDR1-like loop, and the corresponding residue Glu258 of the α 3 domain E strand forms one salt bridge with Arg60 of the cCD8 α 1 C' strand (**Figure 6B**). In contrast, the corresponding residues Arg207 forms two hydrogen bonds with Asp35 of cCD8 α 1, and Glu244 forms one salt bridge with Arg60 of the cCD8 α 2 C' strand in cCD8 $\alpha\alpha$ /pBF2*0401 complex B (**Figure 6B**).

In the α 2 domain of cCD8 $\alpha\alpha$ /pBF2*1501 complex A, Asp104 of the β 4- β 5 loop forms one hydrogen bond with Gln78 of the cCD8 α 1 DE loop, and Asp100 of the β 4 strand contacts to Ser80 of the cCD8 α 1 DE loop with the help of water molecule (**Figure 6A**). However, in cCD8 $\alpha\alpha$ /pBF2*1501 complex B, Glu103 and Asp104 of the β 4- β 5 loop form two hydrogen bonds with Gly79 and Gln78 of the cCD8 α 1 DE loop, and Asp124 of the β 6- β 7 loop forms one hydrogen bond with Arg14 of the cCD8 α 1 AB loop (**Figure 6A**). In cCD8 $\alpha\alpha$ /pBF2*0401 complex A, the residue Arg108 of the β 5 strand forms one hydrogen bond with Glu28 of the CD8 α 1 subunit B strand, Glu103 of the β 4- β 5 loop forms two hydrogen bonds with Gln78 and Gly79 of the cCD8 α 1 DE loop (**Figure 6B**). In contrast, the residue Glu103 and Asp104 of the β 4- β 5 loop form one hydrogen bond with Gly79 and Gln78 of the cCD8 α 1 subunit DE loop respectively, in cCD8 $\alpha\alpha$ /pBF2*0401 complex B (**Figure 6B**). In addition to hydrogen bonds and salt bridges, six van der Waals contacts are contributed by residues of BF2*1501 except for α 3 CD loop and eleven van der Waals contacts are contributed by β 2m to the interaction in cCD8 $\alpha\alpha$ /pBF2*1501 complex A (**Supplementary Table 1**). In cCD8 $\alpha\alpha$ /pBF2*1501 complex B, twelve van der Waals contacts formed by residues of BF2*1501 except for α 3 CD loop and only five van der Waals contacts are contributed by β 2m (**Supplementary Table 1**). Besides forces contributed by the α 3 CD loop, other stable interactions, including hydrogen bonds, salt bridges and van der Waals interactions, that assist in drawing the pBF2*1501 and pBF2*0401 molecules close to cCD8 $\alpha\alpha$ are also mostly different in complex A and complex B. Therefore, the affinity should be different between cCD8 $\alpha\alpha$ and pBF2*1501 and pBF2*0401 in complex A and complex B. In both cases, complex B might possess a higher affinity between cCD8 $\alpha\alpha$ and pBF2*1501 and pBF2*0401 than that of complex A, because more forces including hydrogen bonds and van der Waals interactions predominate between cCD8 $\alpha\alpha$ and pBF2*1501 and pBF2*0401 in complex B (**Table 2**). However, the solvents

might influence the affinity between cCD8 $\alpha\alpha$ and pBF2*1501 in complex A.

Specific Interaction Features Between cCD8 and pMHC-I Outside of Mammals

Complex B of cCD8 $\alpha\alpha$ /pBF2*1501 and complex B of cCD8 $\alpha\alpha$ /pBF2*0401 share a similar CD8 interaction mode with mammalian MHC-I, but the amino acids of BF2*1501 and BF2*0401 especially for the α 3 domain is different from human and mouse pMHC-I molecules (**Figure 2**). Moreover, the amino acid identity of CD8 α is low in chicken, human and mouse (**Figure 2**). These results reveal that chicken cCD8 $\alpha\alpha$ -pMHC-I interaction represents a special feature differing from humans and mice. Corresponding to sequence homology, the interface forces among chicken, human and mouse CD8 $\alpha\alpha$ /pMHC-I showed substantial differences (**Figure 7**). Only two residues, Gln222 and Asp223 of BF2*1501, corresponding to Gln226 and Asp227 in human and mouse MHC-I, and three residues that participate in the complex interaction, Ser39, Tyr54 and Asn104 of cCD8 α , are conserved between chicken and mammals (**Figures 7A, B**).

In the case of hCD8 $\alpha\alpha$ /pHLA-A*0201, mutagenesis of any of the three residues Gln115, Asp122 and Glu128 in the HLA-A*0201 α 2 domain can abolish hCD8 $\alpha\alpha$ binding (37). However, three different residues, Glu103, Asp104 and Asp124, in the BF2*1501 α 2 domain form contacts with cCD8 $\alpha\alpha$ (**Figure 7A**). Moreover, mutagenesis data on the α 3 domain of the human and mouse complexes showed that three clusters of α 3 domain residues (residues 220–232, 233–235, and 245–247) and especially the MHC-I α 3 CD loop (residues 220–228) are key to the CD8 $\alpha\alpha$ -pMHC-I interaction (43, 56). However, in chickens, in addition to Gln222 and Asp223, another five nonconserved residues of BF2*1501, Arg207, Lys215, Val219, Gln225, Ser226, and Glu258, are the main contributors to the interaction with cCD8 $\alpha\alpha$ (**Figures 7A, B**). Among the seven residues, five of them fall into the cluster 220–228, but two residues, Val219 and Gln225, are specific to chickens. Furthermore, Arg207 is located on the BC loop of the BF2*1501 α 3 domain, which is absent in the interactions between CD8 α and HLA-A*0201 and H-2K^b, and no residues of the BC loop participate in the interaction in humans and mice. Another three residues, Lys215, Ser226, and Glu258, are also species specific, although the corresponding residues Glu229 and Gln262 contribute to the interactions in mCD8 $\alpha\alpha$ /pH-2K^b and hCD8 $\alpha\alpha$ /pHLA-A*0201, respectively.

Like the BF2*1501 molecules, most of the contact residues in cCD8 $\alpha\alpha$ are chicken specific. For the cCD8 α 1 subunit, a total of seven residues, namely, Gln78, Gly79, and Arg83 of the DE loop, Arg14 of the AA' loop, Asp35 of the CDR1 loop, Asn104, Gln105 of the CDR3 loop, contribute to the binding to BF2*1501 (**Figure 7A**). In addition to Asn104, six other residues are nonconserved among chicken and human and mouse, and no corresponding residues form contacts in hCD8 α 1 and mCD8 α 1 (**Figures 7A and S1B**). However, three of four contact residues in the CD8 α 2 subunit are conserved among cCD8 α and hCD8 α and mCD8 α , including Ser39, Tyr54 and Asn104, because residues Ser39 and

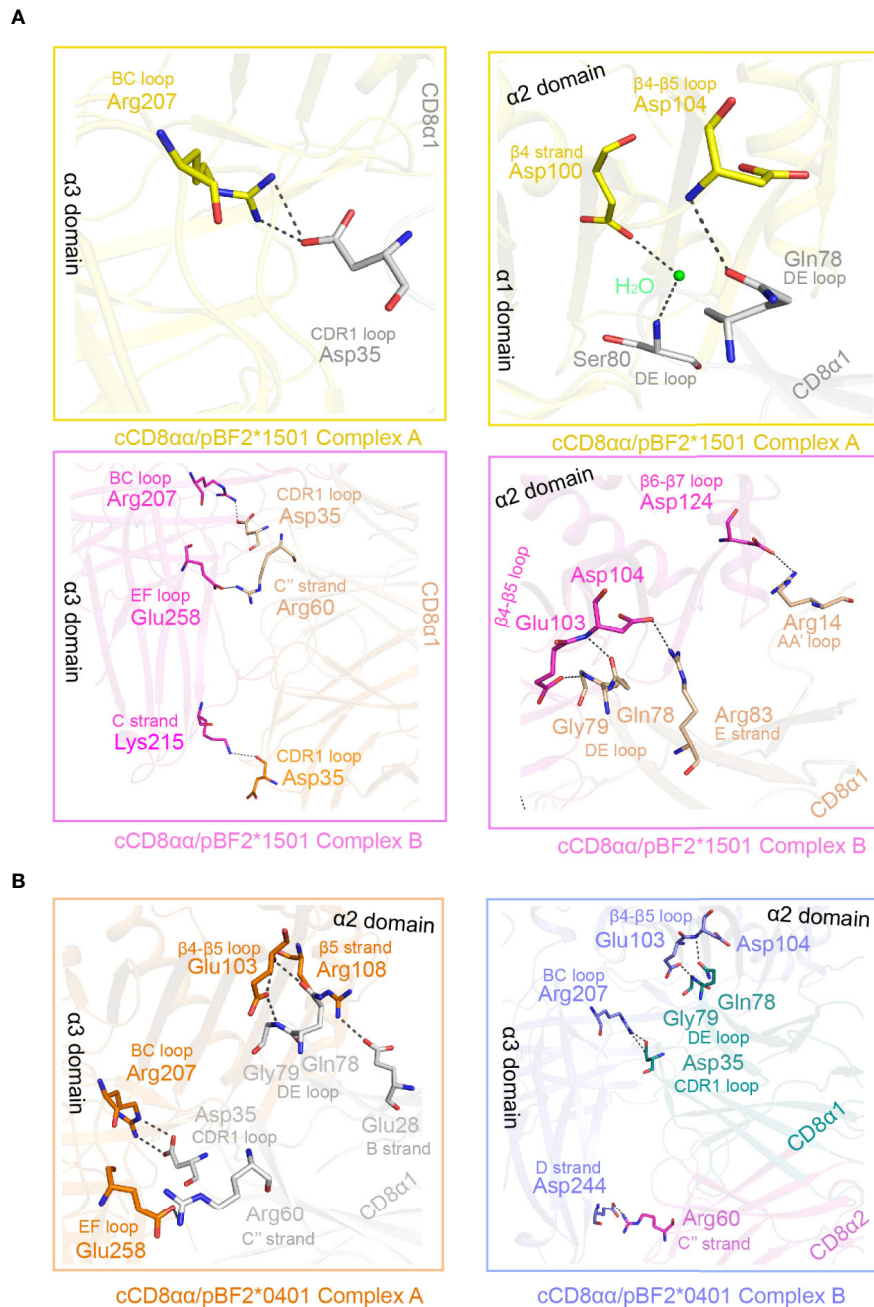
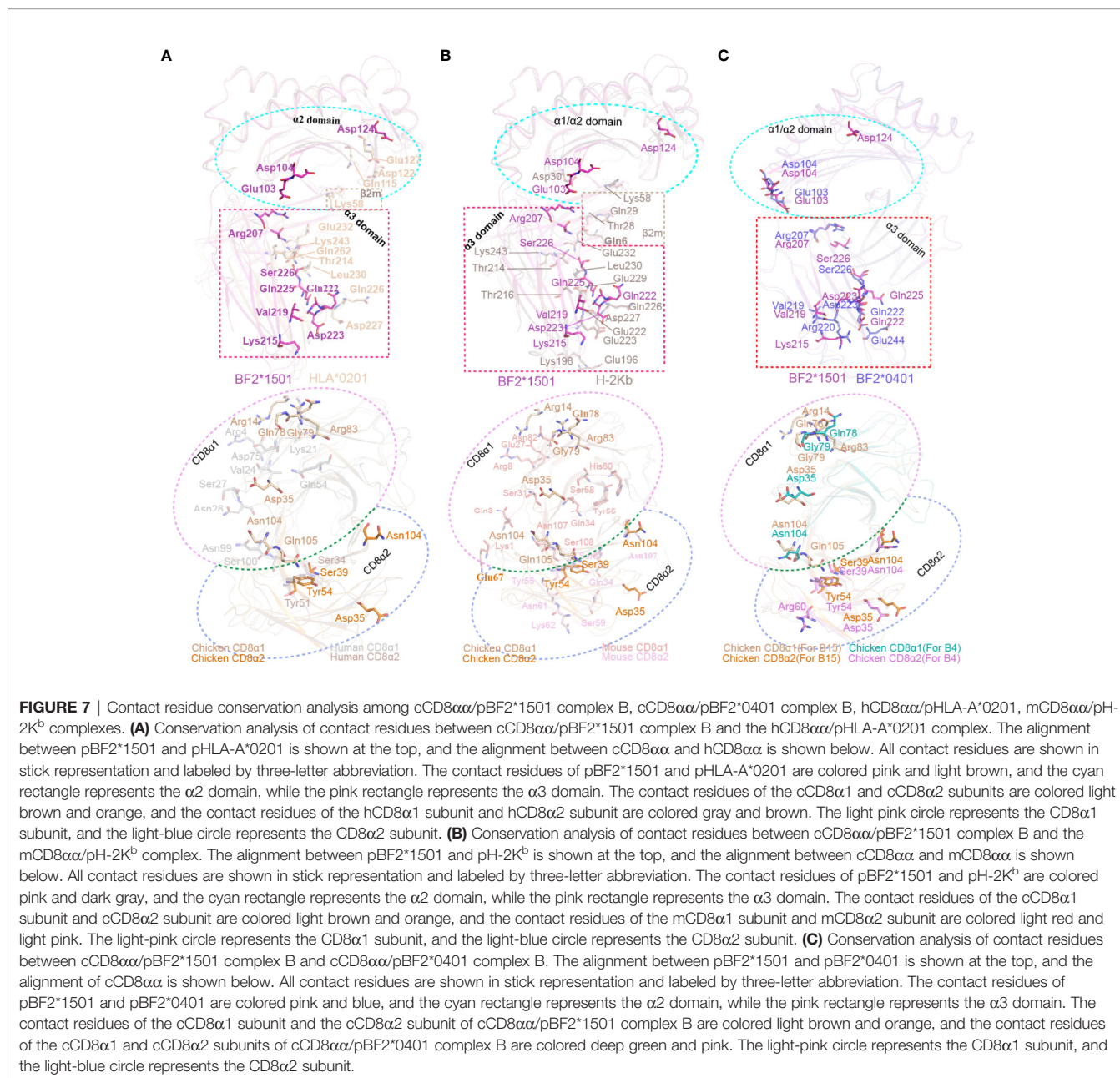


FIGURE 6 | Details of the interaction between the cCD8 $\alpha\alpha$ homodimer and pBF2*1501 and pBF2*0401 of complex A and complex B. **(A)** The interaction between cCD8 $\alpha\alpha$ homodimer and the α 1, α 2, and α 3 domains (exclusive of the CD loop) of pBF2*1501. The interactions of complex A are shown in enlarged views in yellow boxes. The contact residues are marked by sticks and labeled by three-letter abbreviation and sequence number, and the interaction forces are marked by black dotted lines. In complex A, the contact residues of pBF2*1501 are colored yellow, the contact residues of the cCD8 α 1 subunit are colored gray, and the contact residues of the cCD8 α 2 subunit are colored blue. The interactions of complex B are shown in an enlarged view in a pink box. The contact residues are shown in stick representation and labeled by three-letter abbreviation and sequence number, and the interaction forces are marked by black dotted lines. In complex B, the contact residues of pBF2*1501 are colored pink, and the contact residues of the cCD8 α 1 subunit are colored light brown. **(B)** The interaction between the cCD8 $\alpha\alpha$ homodimer and the α 1, α 2, and α 3 domains (exclusive of the CD loop) of pBF2*0401. The interactions of complex A are shown in an enlarged view in an orange box. The contact residues are shown in stick representation and labeled by three-letter abbreviation and sequence number, and the interaction forces are marked by black dotted lines. In complex A, the contact residues of pBF2*0401 are colored orange, and the contact residues of the cCD8 α 1 subunit are colored gray. The interactions of complex B are shown in an enlarged view in a pink box. The contact residues are shown in stick representation and labeled by three-letter abbreviation and sequence number, and the interaction forces are marked by black dotted lines. The contact residues of pBF2*1501 are colored blue, the contact residues of the cCD8 α 1 subunit are colored deep green, and the contact residues of the cCD8 α 2 subunit are colored pink.



Tyr54 form contacts with Gln222, and these interactions are conserved between chicken complex B and the mammalian CD8/pMHC-I complex (**Figures 7A, B**). Another residue, Asp35, of the CDR1 loop is completely species specific in chickens (**Figures 7C and 2B**).

DISCUSSION

The immune molecules of birds, represented by chickens, have low amino acid homology to the corresponding human molecules, but the topological structures of their protein complexes are similar.

However, in essence, the 3D structures of chicken immune molecules have their own species characteristics, which leads to some differences in immunobiology. The current study determined the structures of chicken CD8/pMHC-I complexes for the first time, namely, cCD8 $\alpha\alpha$ /pBF2*1501 and cCD8 $\alpha\alpha$ /pBF2*0401, which each contain complex A and complex B in an asymmetrical unit. cCD8 $\alpha\alpha$ binds to pBF2*1501 and pBF2*0401 in an allele-dependent but peptide-independent manner, as demonstrated by the CD8 $\alpha\alpha$ -pMHC-I interaction in previous studies (38, 39). Remarkably, cCD8 $\alpha\alpha$ binds to pBF2*1501 and pBF2*0401 in complex A of cCD8 $\alpha\alpha$ /pBF2*1501 and cCD8 $\alpha\alpha$ /pBF2*0401 in a novel “face-to-face” mode, which is distinct from

the antibody-like binding mode of the known human and mouse CD8/pMHC-I complexes (19, 35–37). The results showed the heterogeneity of the CTL population and the diversity of its binding with pMHC-I.

Complex B shares the same antibody-like binding mode with the known CD8/pMHC-I complexes in mammals, of which the protruding CD loop was clamped by the CDR loops of cCD8 α . It has been proven that CD8 and TCR cooperatively bind pMHC-I and enhance peptide discrimination (57). The stalk regions of CD8 are interpreted to be highly flexible, but O-glycosylation may significantly restrict the flexibility of the stalks and the mobility of the CD8 head group relative to the T cell membrane (58–60). Therefore, “face-to-face” binding causes the cCD8 α binding orientation to pBF2*1501 and pBF2*0401 to skew towards the α 2 domain and β 2m, which might facilitate larger numbers of $\gamma\delta$ TCR to bind diverse peptides presented by limited BF2 alleles in chicken. No structures of chicken TCR-pMHC-I or TCR-pMHC-I-CD8 are yet available in chickens, but the geometry of the TCR-pMHC-I-CD8 complex could modulate TCR signaling and thereby directly impact T cell development and T cell activity.

Moreover, the “face-to-face” binding mode leads to the loss of most hydrogen bonds and salt bridges between the CD loop of BF2*1501 and BF2*0401 and cCD8 α . However, more water molecules contribute to the interaction between the CD loop of BF2*1501 and BF2*0401 and cCD8 α in complex A. Importantly, the MHC-I α 3 CD loop (residues 220–228) has been proven to be key for the CD8 α -pMHC-I interaction (43, 56). So, these distinct interactions between the CD loop and cCD8 α might result in the different affinity of CD8-pMHC-I interaction in two binding model. Several studies have demonstrated that CD8 can affect the TCR-pMHC-I interaction that determines the consequences of Ag engagement (61–66). Increasing the strength of the CD8-pMHC-I interaction could substantially increase the number of recognized peptides (67). The CD8-pMHC-I interaction strength can optimize the degree of cross-reactivity and Ag sensitivity of CD8 T cells at various stages of their development, and this coreceptor recognition system has coevolved to provide an unparalleled solution to the unique challenges of effective T cell immunity and is necessary to regulate the balance between optimal cross-reactivity and cognate Ag specificity (14). Moreover, it has been reported that O-glycan sialylation of CD8 modulates the affinity for pMHC-I complex binding with little or no effect on the overall structure of CD8 (59, 68). Thus, the antibody-like binding and “face-to-face” binding modes coexist in equilibrium, which might be a “clever” and important strategy that plays an important role in Ag recognition and T cell cross-reactivity during peripheral antigen recognition.

In conclusion, the coexistence of two binding modes in chicken CD8/pMHC-I complexes would be a result of the

molecular arms race between pathogens and chickens, which might enhance the T cell response to major or emerging pathogens, including chicken-derived pathogens that are relevant to human health. This phenomenon might be relevant to the special chicken CTL immune response, especially for the high proportion of approximately 50% of CD8 $^+$ $\gamma\delta$ T cells in peripheral T cells. It is worth emphasizing that chicken CD8 α binding pMHC-I in complex A also provides a new reference model for human T cell therapy.

DATA AVAILABILITY STATEMENT

The coordinates and structural characteristics of pBF2*1501, cCD8 α /pBF2*1501, cCD8 α /pBF2*0401 have been deposited in the Protein Data Bank under accession numbers 6LHF, 6LHG and 6LHH.

AUTHOR CONTRIBUTIONS

YL crystalized the pBF2*1501, cCD8 α /pBF2*1501, and cCD8 α /pBF2*0401 and solved the structures with the help of RC, RL, LZ, BS, and YW. All the research processes were conducted under the supervision of CX. The draft of manuscript was written by YL and revised by JK and CX. All authors contributed to the article and approved the submitted version.

FUNDING

This work was supported by National Natural Science Foundation of China (grant nos.: 31572493 and 31972683).

ACKNOWLEDGMENTS

We thank Professor George F. Gao and Professor Jianxiong Qi of the Institute of Microbiology, Chinese Academy of Sciences, for their excellent suggestions on this study.

SUPPLEMENTARY MATERIAL

The Supplementary Material for this article can be found online at: <https://www.frontiersin.org/articles/10.3389/fimmu.2020.605085/full#supplementary-material>

REFERENCES

- Forsdyke D. Early evolution of MHC polymorphism. *J Theor Biol* (1991) 150:451–6. doi: 10.1016/s0022-5193(05)80439-4
- Germain RN. MHC-dependent antigen processing and peptide presentation: providing ligands for T lymphocyte activation. *Cell* (1994) 76:287–99. doi: 10.1016/0092-8674(94)90336-0
- Jiang N, Huang J, Edwards LJ, Liu B, Zhang Y, Beal CD, et al. Two-stage cooperative T cell receptor-peptide major histocompatibility complex-CD8 trimolecular interactions amplify antigen discrimination. *Immunity* (2011) 34:13–23. doi: 10.1016/j.immuni.2010.12.017
- Cole DK, Laugel B, Clement M, Price DA, Wooldridge L, Sewell AK. The molecular determinants of CD8 co-receptor function. *Immunology* (2012) 137:139–48. doi: 10.1111/j.1365-2567.2012.03625.x

5. Holler PD, Kranz DM. Quantitative analysis of the contribution of TCR/pepMHC affinity and CD8 to T cell activation. *Immunity* (2003) 18:255–64. doi: 10.1016/s1074-7613(03)00019-0
6. Dockree T, Holland CJ, Clement M, Ladell K, McLaren JE, Den Berg HAV, et al. CD8+ T-cell specificity is compromised at a defined MHC I/CD8 affinity threshold. *Immunol Cell Bio* (2017) 95:68–76. doi: 10.1038/icb.2016.85
7. Purbhoo MA, Boulter JM, Price DA, Vuidepot A-L, Hourigan CS, Dunbar PR, et al. The human CD8 coreceptor effects cytotoxic T cell activation and antigen sensitivity primarily by mediating complete phosphorylation of the T cell receptor ζ chain. *J Biol Chem* (2001) 276:32786–92. doi: 10.1074/jbc.M102498200
8. Arcaro A, Grégoire C, Bakker TR, Baldi L, Jordan M, Goffin L, et al. CD8 β endows CD8 with efficient coreceptor function by coupling T cell receptor/CD3 to raft-associated CD8/p56lck complexes. *J Exp Med* (2001) 194:1485–95. doi: 10.1084/jem.194.10.1485
9. Zamoyska R. CD4 and CD8: modulators of T-cell receptor recognition of antigen and of immune responses? *Curr Opin Immunol* (1998) 10:82–7. doi: 10.1016/s0952-7915(98)80036-8
10. Zamoyska R, Derham P, Gorman SD, von Hoegen P, Bolen JB, Veillette A, et al. Inability of CD8 α' polypeptides to associate with p56 lck correlates with impaired function *in vitro* and lack of expression *in vivo*. *Nature* (1989) 342:278. doi: 10.1038/342278a0
11. Veillette A, Bookman MA, Horak EM, Bolen JB. The CD4 and CD8 T cell surface antigens are associated with the internal membrane tyrosine-protein kinase p56lck. *Cell* (1988) 55:301–8. doi: 10.1016/0092-8674(88)90053-0
12. Wilson DB, Wilson DH, Schroder K, Pinilla C, Blondelle S, Houghten RA, et al. Specificity and degeneracy of T cells. *Mol Immunol* (2004) 40:1047–55. doi: 10.1016/j.molimm.2003.11.022
13. Mason D. A very high level of crossreactivity is an essential feature of the T-cell receptor. *Immunol Today* (1998) 19:395–404. doi: 10.1016/s0167-5699(98)01299-7
14. Wooldridge L, Laugel B, Ekeruche J, Clement M, van den Berg HA, Price DA, et al. CD8 controls T cell cross-reactivity. *J Immunol* (2010) 185:4625–32. doi: 10.4049/jimmunol.1001480
15. Yin Y, Mariuzza RA. The multiple mechanisms of T cell receptor cross-reactivity. *Immunity* (2009) 31:849–51. doi: 10.1016/j.immuni.2009.12.002
16. Littman DR. The structure of the CD4 and CD8 genes. *Annu Rev Immunol* (1987) 5:561–84. doi: 10.1146/annurev.iv.05.040187.003021
17. Cheroutre H, Lambolez F. Doubting the TCR coreceptor function of CD8 α alpha. *Immunity* (2008) 28:149–59. doi: 10.1016/j.immuni.2008.01.005
18. Rudolph MG, Stanfield RL, Wilson IA. How TCRs bind MHCs, peptides, and coreceptors. *Annu Rev Immunol* (2006) 24:419–66. doi: 10.1146/annurev.immunol.23.021704.115658
19. Rui Wang KN, Margulies DH. Structural Basis of the CD8 α /MHC Class I Interaction: Focused Recognition Orients CD8 β to a T Cell Proximal Position. *J Immunol* (2009) 183:2554–64. doi: 10.4049/jimmunol.0901276
20. Robert J. Comparative study of tumorigenesis and tumor immunity in invertebrates and nonmammalian vertebrates. *Dev Comp Immunol* (2010) 34:915–25. doi: 10.1016/j.dci.2010.05.011
21. Luhtala M. Chicken CD4, CD8 α beta, and CD8 α alpha T cell co-receptor molecules. *Poult Sci* (1998) 77:1858–73. doi: 10.1093/ps/77.12.1858
22. Erf GF, Bottje WG, Bersi TK. CD4, CD8 and TCR defined T-cell subsets in thymus and spleen of 2- and 7-week old commercial broiler chickens. *Vet Immunol Immunopathol* (1998) 62:339–48. doi: 10.1016/s0165-2427(97)00070-6
23. Davidson NJ, Boyd RL. Delineation of chicken thymocytes by CD3-TCR complex, CD4 and CD8 antigen expression reveals phylogenically conserved and novel thymocyte subsets. *Int Immunol* (1992) 4:1175–82. doi: 10.1093/intimm/4.10.1175
24. Veillette A, Ratcliffe MJ. Avian CD4 and CD8 interact with a cellular tyrosine protein kinase homologous to mammalian p56lck. *Eur J Immunol* (1991) 21:397–401. doi: 10.1002/eji.1830210222
25. Liaw HJ, Chen WR, Huang YC, Tsai CW, Chang KC, Kuo CL. Genomic organization of the chicken CD8 locus reveals a novel family of immunoreceptor genes. *J Immunol* (2007) 178:3023–30. doi: 10.4049/jimmunol.178.5.3023
26. Liu Y, Li X, Qi J, Zhang N, Xia C. The structural basis of chicken, swine and bovine CD8 α alpha dimers provides insight into the co-evolution with MHC I in endotherm species. *Sci Rep* (2016) 6:24788. doi: 10.1038/srep24788
27. Shekhar S, Milling S, Yang X. Migration of gammadelta T cells in steady-state conditions. *Vet Immunol Immunopathol* (2012) 147:1–5. doi: 10.1016/j.vetimm.2012.03.016
28. Hayday AC. [gamma][delta] cells: a right time and a right place for a conserved third way of protection. *Annu Rev Immunol* (2000) 18:975–1026. doi: 10.1146/annurev.immunol.18.1.975
29. Raeesi V, Ehsani A, Torshizi RV, Sargolzaei M, Masoudi AA, Dideban R. Genome-wide association study of cell-mediated immune response in chicken. *J Anim Breed Genet* (2017) 134:405–11. doi: 10.1111/jbg.12265
30. Fenzl L, Göbel TW, Neulen M-L. $\gamma\delta$ T cells represent a major spontaneously cytotoxic cell population in the chicken. *Dev Comp Immunol* (2017) 73:175–83. doi: 10.1016/j.dci.2017.03.028
31. Laursen AMS, Kulkarni RR, Taha-Abdelaziz K, Plattner BL, Read LR, Sharif S. Characterization of gamma delta T cells in Marek's disease virus (Gallid herpesvirus 2) infection of chickens. *Virology* (2018) 522:56–64. doi: 10.1016/j.virol.2018.06.014
32. Arstila TP, Lassila O. Androgen-induced expression of the peripheral blood gamma delta T cell population in the chicken. *J Immunol* (1993) 151:6627–33.
33. Sowder JT, Chen CL, Ager LL, Chan MM, Cooper MD. A large subpopulation of avian T cells express a homologue of the mammalian T gamma/delta receptor. *J Exp Med* (1988) 167:315–22. doi: 10.1084/jem.167.2.315
34. Berndt A, Pieper J, Methner U. Circulating gamma delta T cells in response to Salmonella enterica serovar enteritidis exposure in chickens. *Infect Immun* (2006) 74:3967–78. doi: 10.1128/IAI.01128-05
35. Shi Y, Qi J, Iwamoto A, Gao GF. Plasticity of human CD8 α alpha binding to peptide-HLA-A*2402. *Mol Immunol* (2011) 48:2198–202. doi: 10.1016/j.molimm.2011.05.009
36. Kern PS, Teng MK, Smolyar A, Liu JH, Liu J, Hussey RE, et al. Structural basis of CD8 coreceptor function revealed by crystallographic analysis of a murine CD8 α alpha ectodomain fragment in complex with H-2K^b. *Immunity* (1998) 9:519–30. doi: 10.1016/s1074-7613(00)80635-4
37. Gao GF, Tormo J, Gerth UC, Wyer JR, McMichael AJ, Stuart DII, et al. Crystal structure of the complex between human CD8 α (alpha) and HLA-A2. *Nature* (1997) 387:630–4. doi: 10.1038/42523
38. Huang J, Edwards LJ, Evavold BD, Zhu C. Kinetics of MHC-CD8 interaction at the T cell membrane. *J Immunol* (2007) 179:7653–62. doi: 10.4049/jimmunol.179.11.7653
39. Gao GF, Jakobsen BK. Molecular interactions of coreceptor CD8 and MHC class I: the molecular basis for functional coordination with the T-cell receptor. *Immunol Today* (2000) 21:630–6. doi: 10.4049/jimmunol.179.11.7653
40. Van Laethem F, Sarafova SD, Park JH, Tai X, Pobezinsky L, Guinter TII, et al. Deletion of CD4 and CD8 coreceptors permits generation of alpha beta T cells that recognize antigens independently of the MHC. *Immunity* (2007) 27:735–50. doi: 10.1016/j.immuni.2007.10.007
41. Kaufman J, Andersen R, Avila D, Engberg J, Lambris J, Salomonsen J, et al. Different features of the MHC class I heterodimer have evolved at different rates. Chicken BF and beta 2-microglobulin sequences reveal invariant surface residues. *J Immunol* (1992) 148:1532–46.
42. Liu Y, Xiong Y, Naidenko OV, Liu JH, Zhang R, Joachimiak A, et al. The crystal structure of a TL/CD8 α alpha complex at 2.1 Å resolution: implications for modulation of T cell activation and memory. *Immunity* (2003) 18:205–15. doi: 10.1016/s1074-7613(03)00027-x
43. Salter RD, Benjamin RJ, Wesley PK, Buxton SE, Garrett TP, Clayberger C, et al. A binding site for the T-cell co-receptor CD8 on the alpha 3 domain of HLA-A2. *Nature* (1990) 345:41–6. doi: 10.1038/345041a0
44. Potter TA, Rajan T, Dick RFII, Bluestone JA. Substitution at residue 227 of H-2 class I molecules abrogates recognition by CD8-dependent, but not CD8-independent, cytotoxic T lymphocytes. *Nature* (1989) 337:73. doi: 10.1038/337073a0
45. Hunt HD, Fulton JE. Analysis of polymorphisms in the major expressed class I locus (B-FIV) of the chicken. *Immunogenetics* (1998) 47:456–67. doi: 10.1007/s002510050383
46. Kaufman J. Generalists and specialists: a new view of how MHC class I molecules fight infectious pathogens. *Trends Immunol* (2018) 39:367–79. doi: 10.1016/j.it.2018.01.001

47. Koch M, Camp S, Collen T, Avila D, Salomonsen J, Wallny HJ, et al. Structures of an MHC class I molecule from B21 chickens illustrate promiscuous peptide binding. *Immunity* (2007) 27:885–99. doi: 10.1016/j.immuni.2007.11.007
48. Wallny HJ, Avila D, Hunt LG, Powell TJ, Riegert P, Salomonsen J, et al. Peptide motifs of the single dominantly expressed class I molecule explain the striking MHC-determined response to Rous sarcoma virus in chickens. *Proc Natl Acad Sci U S A* (2006) 103:1434–9. doi: 10.1073/pnas.0507386103
49. Zhang J, Chen Y, Qi J, Gao F, Liu Y, Liu J, et al. Narrow groove and restricted anchors of MHC class I molecule BF2*0401 plus peptide transporter restriction can explain disease susceptibility of B4 chickens. *J Immunol* (2012) 189:4478–87. doi: 10.4049/jimmunol.1200885
50. Sun B, Li X, Wang Z, Xia C. Complex assembly, crystallization and preliminary X-ray crystallographic analysis of the chicken MHC class I molecule BF2*1501. *Acta Crystallogr Sect F Struct Biol Cryst Commun* (2013) 69:122–5. doi: 10.1107/S1744309112050300
51. Corr M, Slanetz AE, Boyd LF, Jelonek MT, Khilko S, al-Ramadi BK, et al. T cell receptor-MHC class I peptide interactions: affinity, kinetics, and specificity. *Science* (1994) 265:946–9. doi: 10.1126/science.7701331
52. Otwinowski, Minor. Processing of X-ray Diffraction Data Collected in Oscillation Mode. *Methods Enzymol* (1997) 276:307–26. doi: 10.1016/S0076-6879(97)76066-X
53. Vaguine AA, Richelle J, Wodak SJ. SFCHECK: a unified set of procedures for evaluating the quality of macromolecular structure-factor data and their agreement with the atomic model. *Acta Crystallogr Sect D Biol Cryst* (1999) 55:191–205. doi: 10.1107/S0907444998006684
54. Hoof I, Peters B, Sidney J, Pedersen LE, Sette A, Lund O, et al. NetMHCpan, a method for MHC class I binding prediction beyond humans. *Immunogenetics* (2009) 61:1–13. doi: 10.1007/s00251-008-0341-z
55. Connolly JM, Hansen TH, Ingold AL, Potter TA. Recognition by CD8 on cytotoxic T lymphocytes is ablated by several substitutions in the class I $\alpha 3$ domain: CD8 and the T-cell receptor recognize the same class I molecule. *Proc Natl Acad Sci USA* (1990) 87:2137–41. doi: 10.1073/pnas.87.6.2137
56. Sekimata M, Tanabe M, Sarai A, Yamamoto J, Kariyone A, Nakauchi H, et al. Different effects of substitutions at residues 224 and 228 of MHC class I on the recognition of CD8. *J Immunol* (1993) 150:4416–26.
57. Jiang N, Huang J, Edwards LJ, Liu B, Zhang Y, Beal CD, et al. Two-Stage Cooperative T Cell Receptor-Peptide Major Histocompatibility Complex-CD8 Trimolecular Interactions Amplify Antigen Discrimination. *Immunity* (2013) 34:13–23. doi: 10.1016/j.immuni.2010.12.017
58. Shore DA, Wilson IA, Dwek RA, Rudd PM. Glycosylation and the function of the T cell co-receptor CD8. *Adv Exp Med Biol* (2005) 564:71–84. doi: 10.1007/0-387-25515-X_12
59. Merry AH, Gilbert RJ, Shore DA, Royle L, Miroshnychenko O, Vuong M, et al. O-glycan sialylation and the structure of the stalk-like region of the T cell co-receptor CD8. *J Biol Chem* (2003) 278:27119–28. doi: 10.1074/jbc.M213056200
60. Li Y, Yin Y, Mariuzza RA. Structural and Biophysical Insights into the Role of CD4 and CD8 in T Cell Activation. *Front Immunol* (2013) 4:206. doi: 10.3389/fimmu.2013.00206
61. van den Berg HA, Wooldridge L, Laugel B, Sewell AK. Coreceptor CD8-driven modulation of T cell antigen receptor specificity. *J Theor Biol* (2007) 249:395–408. doi: 10.1016/j.jtbi.2007.08.002
62. Laugel B, van den Berg HA, Gostick E, Cole DK, Wooldridge L, Boulter J, et al. Different T cell receptor affinity thresholds and CD8 coreceptor dependence govern cytotoxic T lymphocyte activation and tetramer binding properties. *J Biol Chem* (2007) 282:23799–810. doi: 10.1074/jbc.M700976200
63. Wooldridge L, van den Berg HA, Glick M, Gostick E, Laugel B, Hutchinson SL, et al. Interaction between the CD8 coreceptor and major histocompatibility complex class I stabilizes T cell receptor-antigen complexes at the cell surface. *J Biol Chem* (2005) 280:27491–501. doi: 10.1074/jbc.M500555200
64. Gakamsky DM, Luescher IF, Pramanik A, Kopito RB, Lemonnier F, Vogel H, et al. CD8 kinetically promotes ligand binding to the T-cell antigen receptor. *Biophys J* (2005) 89:2121–33. doi: 10.1529/biophysj.105.061671
65. Garcia KC, Scott CA, Brunmark A, Carbone FR, Peterson PA, Wilson IA, et al. CD8 enhances formation of stable T-cell receptor/MHC class I molecule complexes. *Nature* (1996) 384:577–81. doi: 10.1038/384577a0
66. Luescher IF, Vivier E, Leyer A, Mahiou J, Godeau F, Malissen B, et al. CD8 modulation of T-cell antigen receptor-ligand interactions on living cytotoxic T lymphocytes. *Nature* (1995) 373:353–6. doi: 10.1038/373353a0
67. Hutchinson SL, Wooldridge L, Tafuro S, Laugel B, Glick M, Boulter JM, et al. The CD8 T cell coreceptor exhibits disproportionate biological activity at extremely low binding affinities. *J Biol Chem* (2003) 278:24285–93. doi: 10.1074/jbc.M300633200
68. Daniels MA, Devine L, Miller JD, Moser JM, Lukacher AE, Altman JD, et al. CD8 binding to MHC class I molecules is influenced by T cell maturation and glycosylation. *Immunity* (2001) 15:1051–61. doi: 10.1016/s1074-7613(01)00252-7

Conflict of Interest: The authors declare that the research was conducted in the absence of any commercial or financial relationships that could be construed as a potential conflict of interest.

Copyright © 2020 Liu, Chen, Liang, Sun, Wu, Zhang, Kaufman and Xia. This is an open-access article distributed under the terms of the Creative Commons Attribution License (CC BY). The use, distribution or reproduction in other forums is permitted, provided the original author(s) and the copyright owner(s) are credited and that the original publication in this journal is cited, in accordance with accepted academic practice. No use, distribution or reproduction is permitted which does not comply with these terms.